Influence of magnetic relaxation on magnetoelastic resonance-based detection

OPEN ACCESS
IOP Publishing
Journal of Physics D: Applied Physics
J. Phys. D: Appl. Phys. **56** (2023) 105001 (10pp)
https://doi.org/10.1088/1361-6463/acba29

Influence of magnetic relaxation on magnetoelastic resonance-based detection

B Sisniega[1,*], J Gutiérrez[1,2], J M Barandiaran[1], J M Porro[2,3] and A García-Arribas[1,2]

[1] Universidad del País Vasco (UPV/EHU), Leioa 48940, Spain
[2] BCMaterials, Basque Center for Materials, Applications and Nanostructures, Leioa 48940, Spain
[3] Ikerbasque-Basque Foundation for Science, Bilbao 48009, Spain

E-mail: beatriz.sisniega@ehu.eus

Received 19 May 2022, revised 16 January 2023
Accepted for publication 8 February 2023
Published 23 February 2023

Abstract

The phenomenon of magnetic relaxation in amorphous ferromagnetic alloys can result in an undesired time evolution of the magnetization that produces serious drawbacks in the use of these materials in sensor applications. The present work studies, at room temperature, the influence of magnetic relaxation on the performance of an amorphous ferromagnetic ribbon as the main element of a magnetoelastic resonance (MER)-based sensor. The time evolution was observed through the evolution of the MER signal, in particular through the variation experienced by the resonance frequency f_r, which is the main parameter used for sensing. It is found that, after the bias field is changed to a given value, and under constant excitation conditions, f_r increases with time in a typical relaxation behavior with a relaxation amplitude Δf_r and a relaxation time τ that depend on the excitation conditions. The amplitude of the excitation h turned out to be a key factor on the relaxation, since larger excitation field amplitudes ($h \geqslant 100$ mOe) result in a considerable decrease of relaxation times ($\tau < 460$ s) and a reduction of the variation of the resonance frequency ($\Delta f_r < 77$ Hz). The influence of this relaxation on the sensor performance and the possible approaches to overcome this problem are evaluated and applied to the case of a magnetoelastic sensor, operating as mass sensor, for monitoring a chemical precipitation reaction.

Keywords: magnetic relaxation, magnetoelastic resonance, magnetoelastic sensor

(Some figures may appear in colour only in the online journal)

1. Introduction

Magnetoelastic resonance (MER) based sensors are usually made of ribbon-shaped amorphous soft ferromagnetic alloys obtained by melt spinning technique [1]. In these materials, the magnetic and mechanical properties are strongly coupled, so that the material can be mechanically excited with an external alternating magnetic field (due to the magnetostriction), and vice versa: the application of mechanical forces or loads produces changes in its magnetic state (due to the magnetoelasticity). Upon magnetic excitation, the sensor can enter in longitudinal resonance at specific frequencies of excitation f_n, determined by the dimensions and elastic properties of the ribbon, according to the expression:

$$f_n = \frac{n}{2L}\sqrt{\frac{E}{\rho}} \quad (1)$$

* Author to whom any correspondence should be addressed.

where $n = 1$ corresponds to the fundamental resonance frequency, L is the length of the ribbon, ρ its density, and E is the Young´s modulus, which depends on the magnetic state of the material and thus on the applied magnetic bias field (through the so called ΔE effect) [2]. This resonant behavior is highly sensitive to different external parameters, a phenomenon that has led to the use of these materials in a wide variety of sensing systems [3–11], including other applications as electronic surveillance sensors [12], and, to a less extent, cell monitoring [13, 14], and frost [15] and gas detection [16, 17].

One of the main advantages of such sensors is the contactless operation. In most applications the sensing parameter is just the resonant frequency, which is also a rather easy parameter to be measured with high accuracy. For instance, in mass change detection, a small increment of mass, Δm, uniformly distributed over the ribbon of mass m_0, produces, to a second order approximation, an expected resonant frequency shift Δf of [3]:

$$\frac{\Delta f}{f_0} \approx -\frac{1}{2}\left(\frac{\Delta m}{m_0}\right) + \frac{3}{8}\left(\frac{\Delta m}{m_0}\right)^2 \qquad (2)$$

In this case, the ultimate resolution of the sensor is determined by the frequency resolution that can be achieved with the measuring system. It is possible to attain a few hertz resolution measuring a resonant frequency of, say, 100 kHz, so that a resolution of a few tens of ppm, relative to the sensor mass, is possible. More specifically, for a typical sensor with a mass of about 10 mg, the ultimate sensitivity of the sensor will be of the order of the micrograms.

The above characteristics, specially contactless detection, make MER sensors gain advantage as compared with other sensor types, as electrochemical, quartz balances and so on [3].

Although amorphous soft magnetic materials present excellent mechanical and magnetic properties for its use in sensor applications [18, 19], they are not completely free of issues, as temperature and time instabilities of their properties. Due to their production method, which forces them to undergo ultra-fast cooling from a liquid phase, amorphous materials are not in thermodynamic equilibrium. Actually, they are in a meta-stable state, which is the origin of relaxation phenomena, also called disaccommodation or magnetic after-effect, leading to changes of their magnetic properties, even at room temperature.

As an example of the negative effect of magnetic relaxation on the performance of MER sensors, figure 1 presents the results obtained by a magnetoelastic sensor used to monitor in real time the precipitation reaction of calcium oxalate (CaC_2O_4) crystals. The experiment is described in detail in [10, 20]. The sensor resonance frequency was monitored as a function of time while the precipitate from the reaction between $CaCl_2$ and $H_2C_2O_4$ settles on the sensor, increasing the total mass of the resonator and therefore decreasing its resonance frequency, as described by equation (2). Figure 1 shows the changes in the resonance frequency of the sensor for two experiments using different concentrations of the reagents: 1 mili-Molar (1 mM) and 3 mM. Contrary to what is expected, the resonance frequency shows an initial increase before starting to decrease. The anomalous behavior is caused by the magnetic relaxation effect. In the case of 1 mM concentration, the resonance frequency is greater than the initial f_r at all times up to 2000 s, a behavior that should correspond to a decrease of mass instead of a precipitation process. For 3 mM concentration, the effect is not as radical, and a final decrease of f_r of around 60 Hz is shown, but still a distortion of the precipitated mass is evident at short times, because of the initial increase of the resonance frequency. A control run, performed with no reagents in the solution, shows a large effect of the relaxation (which increases the resonance frequency by more than 30 Hz). Such relaxation overlaps with the precipitation and does not allow a reliable operation of the sensor.

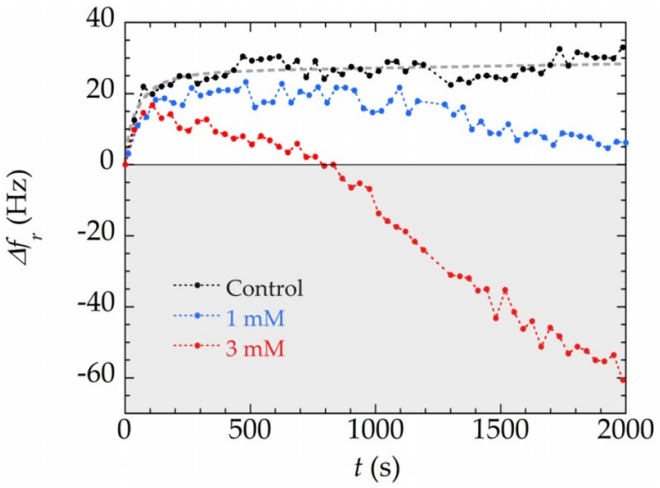

Figure 1. Change of the resonance frequency of the sensor as the precipitate (CaC_2O_4) forms. Blue dots correspond to 1 mM concentration of the reagents and red ones to 3 mM. The control measurement is represented with black dots. The grey dashed line is used to correct the relaxation effect (see section 4.4).

2. Magnetic relaxation in metallic glasses

Magnetic relaxation, disaccommodation or after-effect is a well known effect since the 50's of the last century [21, 22]. The basic effect occurs when a magnetic field is applied to a magnetic material. The magnetization and susceptibility do not reach their final values immediately after the field is applied, but some time is needed for the material to relax into a thermal equilibrium state. The characterization of magnetic relaxation is usually performed by following such magnitudes after demagnetization [23–25]. This relaxation has been explained in terms of a diffusive ordering mechanism of magnetic defects interacting with the local magnetization, arising after a sudden rearrangement of the magnetic domain structure (as it happens when a magnetic field is suddenly applied or suppressed) [21, 26–29]. Such an effect was soon recognized as a drawback in certain applications, where stable

properties are required for a proper performance. In amorphous magnetic alloys the influence of relaxation has been detected in some parameters used in sensing applications, as the magnetoimpedance [28, 29]. Nevertheless, little information about this issue can be found in MER sensors, where, usually, magnetic relaxation has not been taken into account. However, as seen before, a detailed study of the influence of this phenomenon is basic to assess the sensor performance.

Bearing this in mind, we undertake a thorough study concerning the influence of the magnetic relaxation in the performance of an Fe-rich amorphous magnetoelastic ribbon as sensing material. We have continuously monitored the MER curves and, in particular, the value of the resonance frequency, under the simultaneous application of both alternating and DC-bias magnetic fields. As we will show in the following, magnetic relaxation clearly affects the temporal evolution of the resonance frequency and, therefore, the sensor performance. By analyzing the results, we can establish the operating conditions for best performance of magnetoelastic sensors.

Finally, as a side result, the present study shows also the potential of the MER as a new and accurate method for basic studies of the relaxation in magnetoelastic materials, with high accuracy and resolution.

3. Measurement methodology

Relaxation measurements were carried out by monitoring the resonance signal of a magnetoelastic sensor during a time interval of 2000 s while the parameters of the measurement (DC-bias field, excitation field, temperature, and, in general, all the measurement system configuration) remained stable, so that the changes observed in the sensor signal could not be attributed to variations in these parameters.

The experimental setup to carry out the magnetoelastic measurements (figure 2) consists of a pair of Helmholtz coils producing a constant field longitudinal to the ribbon axis which biases the material (powered by a KIKUSUI Bipolar Power Supply PBZ40-10), and an interrogation coil that produces the alternating magnetic field to magnetostrictively excite the sample and that, in turn, detects the magnetization oscillations induced in the material (from which the MER response was obtained). The magnetoelastic sensor is placed inside the interrogation coil and an impedance analyzer (Keysight, E4990A, 20 Hz–10 MHz) is used to produce the excitation of the material in a range of frequencies and receive the corresponding voltage induced by the magnetic oscillations. The amplitude of the exciting field h was calculated by measuring the current flowing through the calibrated interrogation coil (84.6 Oe A^{-1}) using a current probe (Tek CT-2).

The resonance curves and their corresponding resonance frequencies were measured using the built-in analysis procedures of the analyzer and transmitted to a control computer. The constant bias field H was controlled with a data acquisition device (NI USB-6259) and continuously monitored with a Gaussmeter (Lakeshore, 475 DSP Gaussmeter). The experiments were carried out at room temperature, monitored to be

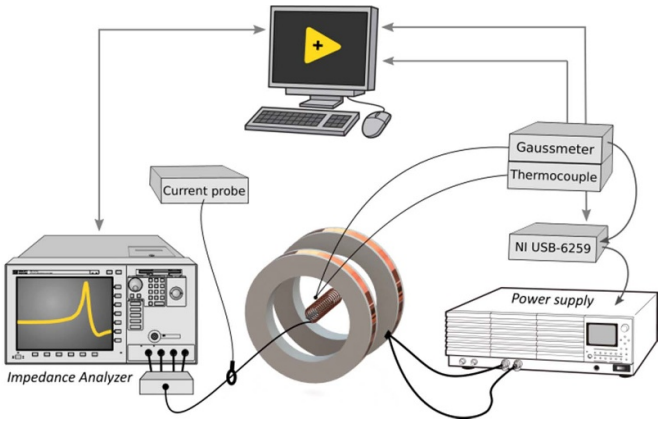

Figure 2. Scheme of the experimental setup used to measure relaxation on magnetoelastic resonance.

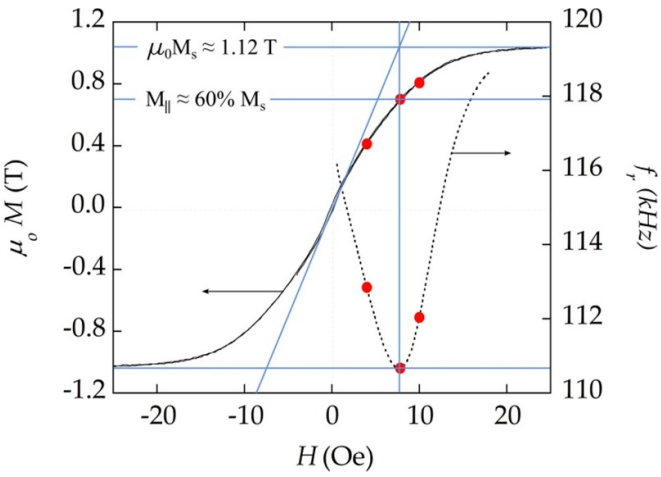

Figure 3. Hysteresis loop of the material (solid line) and dependence of the resonance frequency on the applied bias field (dashed line). Dots indicate the bias field values H selected for the relaxation measurements. Blue lines determine the magnetization at the anisotropy field (see section 4.3).

stable (with variations below 0.1 °C) during the experiments using a thermocouple (NI USB-TC01, type K) inside the measurement system.

The relaxation measurements were performed at three different DC-bias fields H produced by the Helmholtz pair: 4, 7.8 and 10 Oe; and four different amplitudes of the exciting field h produced by the interrogation coil: 20, 42, 100 and 180 mOe respectively.

The material used in the investigation is a magnetoelastic ribbon with composition $Fe_{73}Cr_5Si_{10}B_{12}$ (saturation magnetostriction $\lambda_s = 14$ ppm, saturation magnetization $M_s =$ 1.12 T) [30] (provided by Vacuumschmelze GmbH & Co. KG, Hanau Germany) fabricated using the melt spinning technique. The ribbons were laser-cut to dimensions of 20 mm × 2 mm × 25 μm, with a total weight of about 8 mg. The magnetization curve of the ribbon is shown in figure 3 together with the dependence of its resonance frequency on the applied bias field H (or ΔE effect). Dots represent the bias

field values selected for the magnetic relaxation experiments. Based on previous studies [31–33], the field at which the resonance frequency is minimum, about 7.8 Oe, is considered as the effective value of the anisotropy field of the ribbon, which, in turn, corresponds to the extrapolation of the initial part of the *M (H)* curve.

In order to improve the accuracy in the determination of f_r, the measured resonance curves were numerically fitted to an analytical expression describing the frequency response of the system [34]:

$$Z(f) = Z_0 \left[1 - \frac{8k^2}{\pi^2} \left(1 - \frac{f_1^2}{f^2} + jQ^{-1}\frac{f_1}{f} \right)^{-1} \right] \qquad (3)$$

where $j = \sqrt{-1}$ and the fitted parameters are f_1 (resonance frequency of the main mode, $n = 1$, of oscillation), Z_0 (amplitude of the signal), k (magnetoelastic coupling coefficient) and Q (damping coefficient). The values of the resonance frequency f_r were extracted from the maximum of the fitted curves, resulting in a considerable increase in the consistency of the determination of this parameter.

4. Results and discussion

4.1. Relaxation measurements

An example of the time evolution of the resonance signal of the magnetoelastic sensor under constant bias field is depicted in figure 4(a). At $t = 0$ s, the bias field is set at its desired value ($H = 10$ Oe in this case). After that, due to the relaxation of the magnetization towards the equilibrium value, the resonance curve experiences a frequency shift in both resonance (maximum) and anti-resonance (minimum) frequencies, which shift towards higher values, together with an increase of its amplitude. The time evolution of resonance and anti-resonance frequencies is represented in figure 4(b). The amplitude of the excitation field, $h = 20$ mOe, is maintained constant through the test. Exhaustive experiments revealed that this frequency drift is repetitive, and always takes place whenever a new bias field is applied to the ribbon i.e. when the magnetic domain structure of the material changes, regardless of the initial value of the magnetic field.

In figure 5, the increment (change with respect to its initial value) of the resonance frequency f_r of the sensor during the measurement time (2000 s) is shown for the different values of the excitation h and bias H fields. Dots appearing in figure 5 correspond to the experimental resonance frequencies obtained from the measured curves by numerical fitting to equation (3). As it can be observed f_r increases with time in all cases, up to 0.24% of its initial value in the case of a bias field of 4 Oe and an excitation amplitude of 20 mOe. In a true device, this change of about 270 Hz in the resonance frequency would appear as a time-drift of the output, representing a considerable source of error that would affect the detection accuracy of the sensor.

The tendency observed in the experimental measurements of this phenomenon shows that the change in the resonance

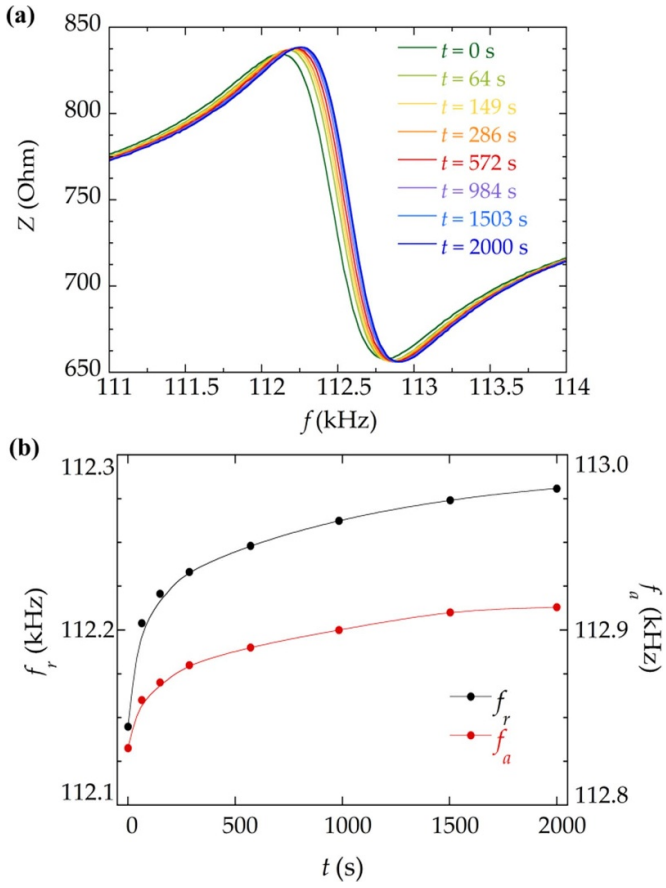

Figure 4. (a) Changes produced in the resonance signal of the sensor due to magnetic relaxation during the measurement under a constant bias field of 10 Oe and excitation amplitude of 20 mOe (each curve corresponds to a different time, from the beginning of the measurement, when the bias field is set, up to 2000 s). (b) Temporal evolution of the resonance f_r and anti-resonance f_a frequencies during relaxation corresponding to the curves shown in (a), obtained from the numerical fitting of the curves to equation (3).

frequency due to the relaxation is more significant in the cases in which the excitation amplitude is weaker. In addition, the phenomenon is more noticeable at lower bias fields, as reported also in [35], below the anisotropy field value, when magnetization occurs mainly due to domain-wall motion, the slope of the hysteresis loop is greater, and small changes of the applied field lead to great changes in magnetization (see figure 3). Relaxation effects decrease for higher applied fields, where the magnetization process is governed by domain rotation. This sensitivity of the relaxation amplitude on the type of magnetization process has been already observed in amorphous alloys, being the relaxation intensity reduced when magnetization reversal occurs mainly by rotation processes [36].

As observed, the magnetic relaxation clearly affects the magnetoelastic sensor signal, causing considerable changes on its resonance frequency that could hide the changes produced by the parameter to be detected, which often causes smaller resonance frequency shifts. The characterization of this relaxation behavior is then fundamental to ensure the stability of the sensor properties at working conditions, and to optimize the

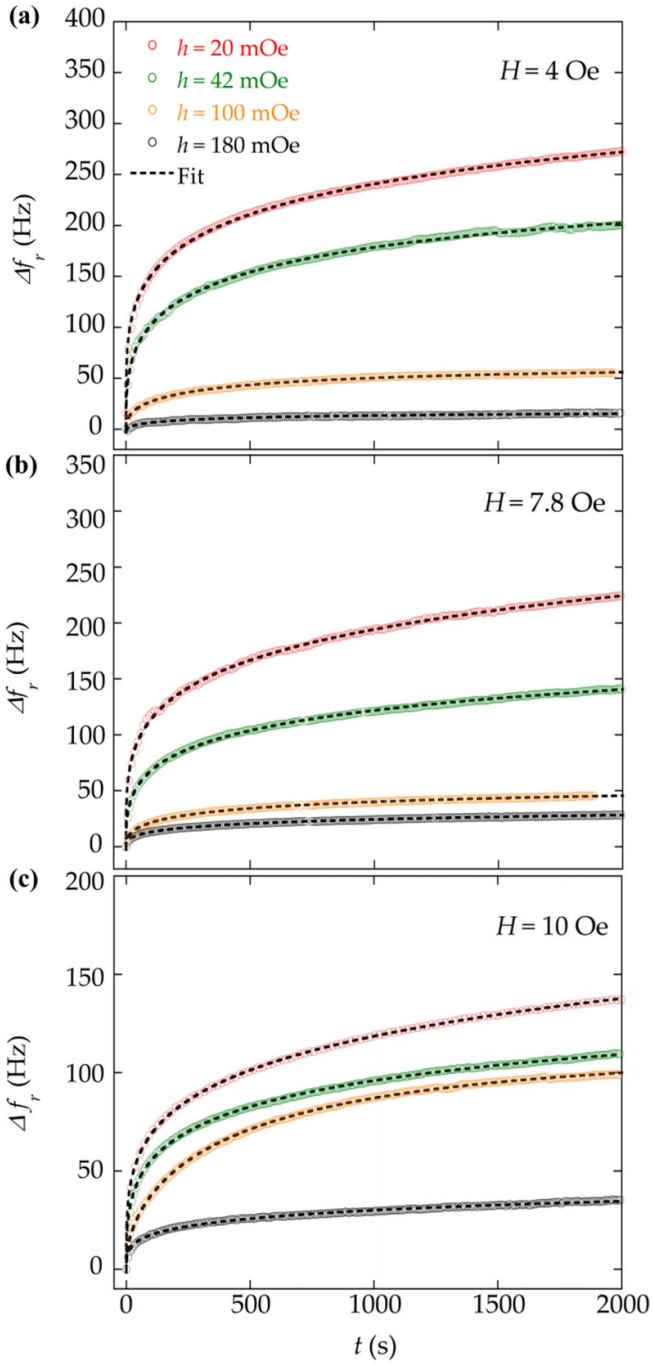

Figure 5. Increment of the resonance frequency of the sensor (dots) and corresponding numerical fitting to expression (4) (dashed lines) for different excitation amplitudes ($h = 20$, 42, 100, 180 mOe) due to magnetic relaxation under the application of constant bias field of (a) 4 Oe; (b) 7.8 Oe (effective anisotropy field); (c) 10 Oe.

operational parameters in order to find a compromise between this stability and the sensor performance.

In order to study in detail the parameters that characterize the relaxation in these materials, the temporal evolution of the resonance frequency f_r was fitted to the following expression, which describes the relaxation behavior and is derived from the formalism of strongly correlated systems (as ferromagnetic systems) [25]:

$$f_r(t) = f_{r_0} + I\left[1 - e^{-\left(t/\tau\right)^{1-n}}\right] \tag{4}$$

where f_{r_0} is the resonance frequency of the magnetoelastic sensor at the initial time, I accounts for the amplitude of the relaxation, τ is the relaxation time, and n is called the coupling parameter that accounts for the correlation of the system. This function is also known in the literature as the stretched exponential, which was first introduced to describe relaxation processes in dielectric materials [37]. The numerical fits were performed using a non-linear least squares fitting in MATLAB®, and the results are in good accordance with the experimental data (as shown in figure 5, dashed black lines). The evolution of the parameters fitted to equation (4) was then analyzed as a function of the excitation amplitude (figure 6).

It is found that the relaxation amplitude parameter I and the relaxation time τ, both decrease with the increase of the excitation amplitude h. The relaxation time decreases from values of up to 2300 s to values of over 300 s. This reduction of the relaxation times suggests that the energy supplied by the excitation (calculated as $E_{mag} = \int hB\mathrm{d}V$ to be of the order of $(0.3 - 6) \times 10^{-9}$J), added to the thermal energy, helps the system to relax faster. As the temperature (and therefore the thermal energy) is the same in all the experiments, the energy provided by the application of the exciting magnetic field drives the changes in the relaxation kinetics.

In a similar manner, the relaxation amplitude I decreases from a value of about 420 Hz to about 30 Hz when the excitation is increased. This decrease of the after-effect intensity with the increase on the amplitude of the driving field has already been pointed out by other authors [38, 39]. It should also be noted that, at low excitation amplitudes, the relaxation amplitude is larger for smaller bias fields H, as previously observed directly in the experimental data (see figure 5).

The coupling parameter n follows a similar trend, indicating a decay of the correlation of the system with increasing excitation amplitudes, being this decay more pronounced in the case of lower bias fields (see figure 6(c)). Apparently, it seems that there is a connection between the degree of correlation of the system and the intensity of the magnetic relaxation, being the reduction in the correlation related with a decrease of the magnetization relaxation behavior.

4.2. Influence of the excitation amplitude on the resonance signal

The amplitude of the excitation has an evident influence on the relaxation effect observed in the behavior of the MER. Further, it also has a direct effect on the intrinsic value of the resonance frequency, considered as the frequency of the maximum of the resonance curve, and on the magnitude of the resonance. Figure 7 compiles the value of both parameters as a function of the bias field H for different excitation amplitudes ($h = 20$, 42, 100, 180 mOe). These measurements were obtained by performing a quick sweep of the bias field, that is, without allowing the magnetization to relax.

It is observed that, as the excitation amplitude increases, both f_r and the amplitude of the resonance decrease. Above the

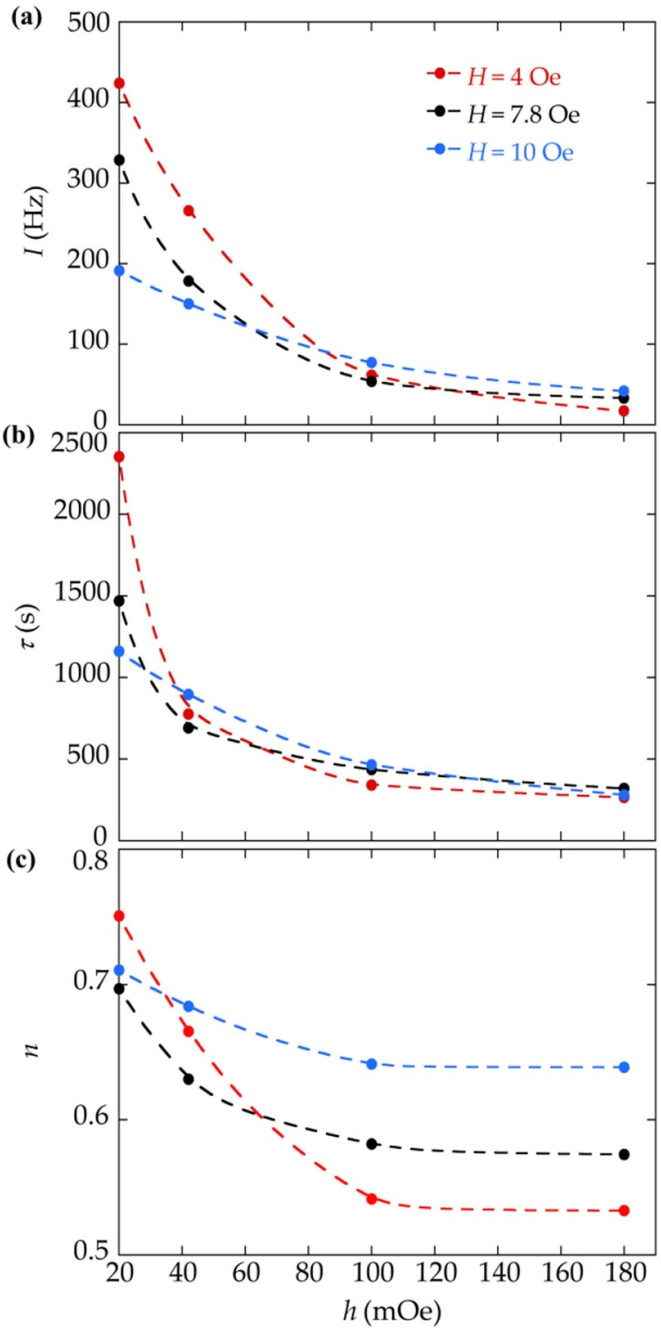

Figure 6. Evolution of the fitted parameters as a function of the amplitude of the exciting field h for different values of the applied DC-bias field ($H = 4$, 7.8 and 10 Oe): (a) relaxation amplitude I, (b) relaxation time τ, and (c) coupling parameter n.

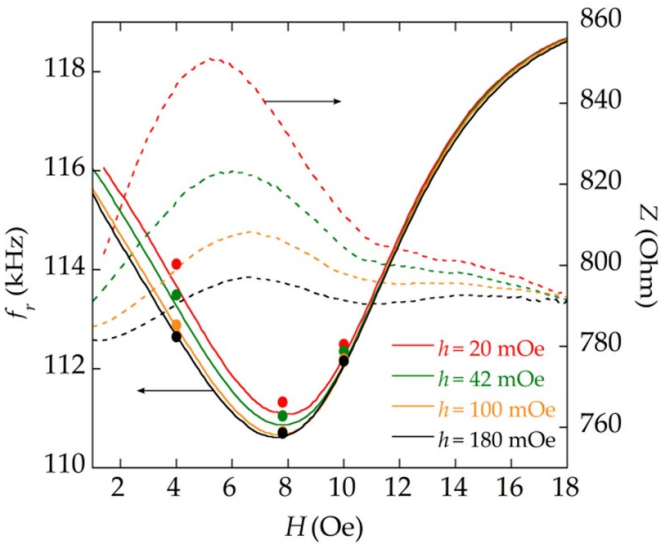

Figure 7. Influence of the bias field on the resonance frequency (solid lines) and maximum impedance (dashed lines) of the resonance curves for different values of the excitation amplitude h. Dots correspond to the relaxed values of the resonance frequency (calculated through the parameters fitted to equation (4)) for the different excitations and bias fields selected in the relaxation measurements.

effective anisotropy field ($H = 7.$ Oe), where the minimum of f_r is reached, the differences in the resonance frequency are greatly reduced. The bias field at which the maximum value of the amplitude is reached is shifted towards higher fields as the excitation increases. These effects have been related to the increase in nonlinear effects in the magnetoelastic response when increasing the excitation amplitude [40]. They are a consequence of the dependence of the magnetoelastic coupling on the magnetization of the material. Larger excitation amplitudes mix different magnetic states, resulting into an increase of the non-linear effects. For low bias fields, the change in magnetization caused by the excitation is much larger than for bias fields close to the knee of the magnetization curve. Overall, this non-linear behavior causes a distortion of the resonance curve [40]. Thus, the ΔE curves are different for different excitation amplitudes as revealed in figure 7.

Given these observations, when selecting a suitable excitation amplitude for a sensing application based on changes of the magnetoelastic frequency, it must be ensured that it does not compromise the quality of the signal and, in addition, it must be considered that the selection will affect the bias field (working point) that must be chosen for an optimum sensor operation. In the case of the material under study, excitation amplitudes $h \geqslant 100$ mOe significantly improve the performance of the sensor, reducing the influence of the relaxation (as already discussed in section 4.1), whereas the bias field should be chosen close to $H = 7$ Oe, where the maximum amplitude of the resonance is obtained.

In order to complete figure 7, we have included the asymptotic values of the resonance frequency after the relaxation is completed (limit at $t \to \infty$ of equation (4)), for the different excitation amplitudes and bias fields (dots in the figure). They reflect the results stated previously: due to magnetic relaxation, f_r changes to a greater extent for low excitation amplitudes and lower bias fields. Concomitantly, the ΔE curve corresponding to the relaxed state is significantly different to that obtained without waiting for the relaxation, which corresponds to solid lines in figure 7.

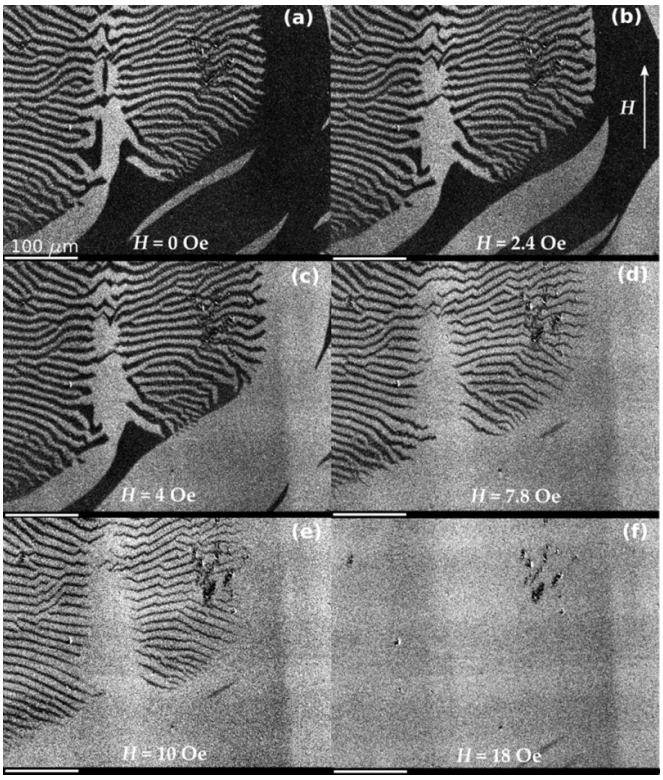

Figure 8. Kerr effect magnetic domain images of a representative zone of the surface of the ribbon at different applied fields (applied in the longitudinal direction of the ribbon): (a) 0 Oe, (b) 2.4 Oe, (c) 4 Oe, (d) 7.8 Oe, (e) 10 Oe and (f) 18 Oe.

4.3. Magnetic domain structure analysis

The magnetic domain structure of the ribbon was analyzed by longitudinal magneto-optical Kerr effect. The Kerr effect images (see figure 8) show a complex domain structure, characteristic of amorphous ferromagnetic ribbons in as-quenched state. The images exemplify the two kinds of patterns found: wide domains with the magnetization in-plane and regions of narrow fingerprint patterns (maze domains or stress patterns, due to melt spinning fabrication), which indicate an easy direction perpendicular to the surface [41]. The Kerr microscopy images shown here are representative of the whole sample of the sensor and of the other pieces of the same cast ribbon. Early studies determined that the intrinsic anisotropy in amorphous magnetic ribbons was due to defects and quenched-in stresses, via magnetoelastic coupling [42, 43]. However, we assume that defects are scarce for the large domain zone and the initial anisotropy associated to them is mainly due to form effects, as those zones, lying between maze domains with perpendicular anisotropy, are quite narrow along the ribbon length. The relative surface of the in-plane and maze domains is about 50/50%. However, regarding volume distribution, the in-plane magnetization as derived from the extrapolation of the initial part of the *M (H)* curve, is about 60% of the saturation (see figure 3). This indicates that the maze domains do not cover the full thickness of the ribbon. A scheme of the magnetic domain structure of the ribbons can be found in an early work (see, for instance, figure 2(a) in [42]).

As it is observed in figure 8, the main changes in the magnetic domain structure occur at low bias fields (figures 8(a)–(c)), where there is a significant movement of walls while wide domains grow. On the other side, for higher fields (figures 8(d) and (e)), the domain structure remains essentially unchanged (stress patterns remain), evolving slowly with the field, and rotation processes dominate over domain wall motion. These pictures directly correlate with the observed magnetic relaxation of the material, since at low fields where the relaxation is higher, most of the domain wall movements occur. Since the origin of magnetic relaxation is based in sudden rearrangements of the magnetic domain structure in the material [21, 26, 27], our magnetic domain observations fully support the measured relaxation magnitude of the MER frequency.

4.4. Sensor operation under magnetic relaxation

As explained above, the magnetic relaxation affects the operation of magnetoelastic-resonance sensors. It can be possible, in principle, to correct the results from the frequency drift caused by the relaxation. Returning to the example described in the introduction (see figure 1), we can subtract the relaxation effect from the measured values, by fitting the control run to expression (4). This fitting is shown in figure 1 as a grey dashed line. In this way, the 'true' resonance frequency is recovered and the sensor performance is enhanced, as shown in figure 9(a).

Indeed, using the mass calibration of the sensor ($\Delta f_r = a_1\Delta m + a_2(\Delta m)^2$, with $a_1 = -9.8 \pm 0.4\,\mathrm{kHz}/mg$, and) obtained in [20], the changes in f_r can be directly correlated

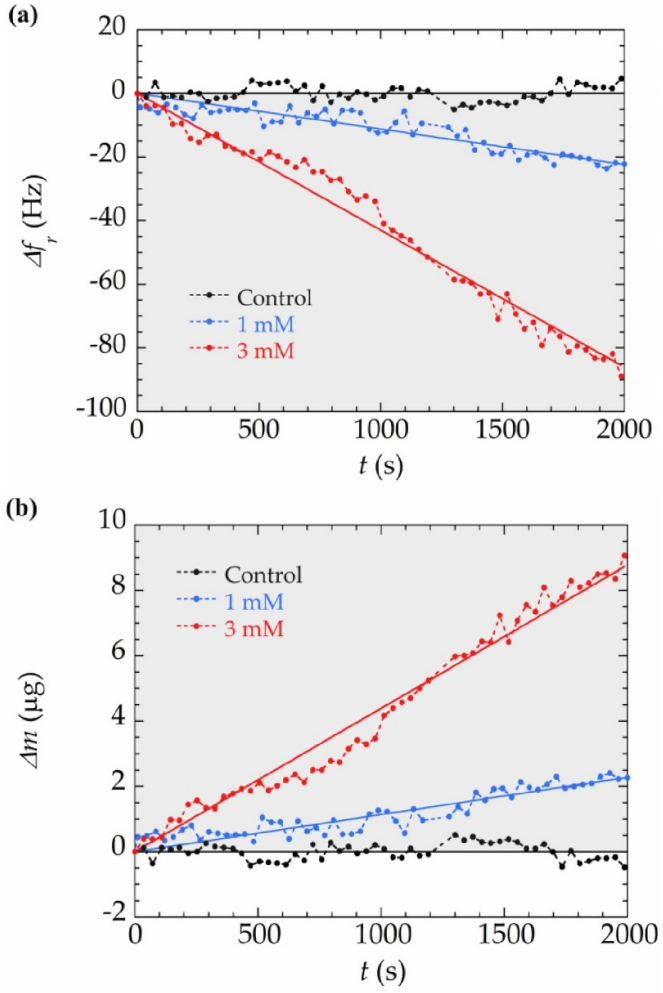

Figure 9. (a) Change of frequency and (b) estimated increment of the sensor mass during the measurement of CaC_2O_4 precipitation, after correction of the magnetic relaxation. As seen, a sensitivity below 1 μg is achieved.

to the corresponding increase in sensor mass, that is, the mass of calcium oxalate precipitate. The results are shown in figure 9(b). As can be observed, with the corrected data, mass differences below $1\mu g$ can be easily resolved, which is in accordance to the conceptual limit discussed in the introduction.

For a rapid operation of the sensor, however, it is much more convenient to use a sensor excitation and bias field which minimize the relaxation amplitude. Following the previously observed results, the bias field at, or below the anisotropy field, and excitations of moderate amplitudes ($h \geqslant 100$ mOe) are, in general, suitable for measuring with low relaxation times and amplitudes, and avoiding the need for corrections of the measured data.

5. Conclusions

In the present study, we investigate the magnetic relaxation behavior that takes place in amorphous ferromagnetic ribbons when they are used as magnetoelastic sensors. The study reveals that the effect of this relaxation on the sensor signal is considerable under certain conditions of the experiment, being the amplitude of the excitation a key factor that influences this process. Using an excitation amplitude of $h = 20$ mOe, relaxation times of about $\tau = 2300$ s and relaxation amplitudes of up to $I = 420$ Hz (for applied bias field of 4 Oe) are observed. It is fundamental, therefore, to select the excitation and the operation point (bias field) in order to minimize the effect of the magnetic relaxation on the magnetoelastic sensor, always taking into account the compromise with the quality of the signal (as discussed in section 4.2). It can be said that moderate excitation amplitudes ($h \geqslant 100$ mOe) are, in general, suitable for measuring with these sensors, resulting in reasonably low relaxation times and relaxation amplitudes ($\tau < 460$ s, $I < 77$ Hz). Depending on the specific interest of each application, it will be necessary to evaluate whether to give priority to the speed of the measurement or, on the contrary, to the precision in the determination of the change in the resonance frequency associated with the measurement. If the measurement requires it, and the experimental procedure allows it, it could be convenient to wait a certain time (relaxation time) for the magnetization to relax in order to be able to make accurate quantitative measurements, which would be in this case less perturbed by this effect. Alternatively, if a post-processing is feasible, it can be possible to fit the sensor blank behavior and subtract the relaxation in the operation conditions. It has been shown that this approach allows to reach the expected resolution of 1 μg in the mass detection experiment of CaC_2O_4 precipitation performed in this study. In addition, annealing treatments of the amorphous ribbons have demonstrated to reduce the magnetic relaxation, as reported in several studies [24, 25], by relaxing the material reducing its density of structural defects and internal stress regions (disappearance of stress pattern domains) [36]. These treatments should be taken into account when using these materials as magnetoelastic sensors if good performance is to be achieved.

Finally, as the resonance frequency of these sensors has been found to be very sensitive to this phenomenon, the measurements of magnetic relaxation performed by MER provide a novel, simple and accurate method of general interest to be employed in the study of magnetic relaxation processes of amorphous ferromagnetic materials.

Data availability statement

The data that support the findings of this study are available upon reasonable request from the authors.

Acknowledgments

The authors would like to thank the financial support from the Basque Government under μ4IIOT project (KK-2021/00082, Elkartek program) and the University Basque Research Groups Funding under Grant IT1479-22. Beatriz Sisniega acknowledges the financial support from the Basque Government through FPI Grant PRE_2021_2_0145.

ORCID iDs

B Sisniega https://orcid.org/0000-0001-6212-7291
J Gutiérrez https://orcid.org/0000-0003-1074-3097
J M Barandiaran https://orcid.org/0000-0002-5402-9314
J M Porro https://orcid.org/0000-0002-8610-9802
A García-Arribas https://orcid.org/0000-0003-1580-0302

References

[1] Savage H T and Wun-fogle M 1994 Amorphous magnetoelastic materials *MRS Online Proc. Libr.* **360** 201–12
[2] Livingston J D 1982 Magnetomechanical properties of amorphous metals *Phys. Status Solidi* a **70** 591–6
[3] Grimes C A, Ong K G, Loiselle K, Stoyanov P G, Kouzoudis D, Liu Y, Tong C and Tefiku F 1999 Magnetoelastic sensors for remote query environmental monitoring *Smart Mater. Struct.* **8** 639
[4] Grimes C A and Kouzoudis D 2000 Remote query measurement of pressure, fluid-flow velocity, and humidity using magnetoelastic thick-film sensors *Sens. Actuators* A **84** 205–12
[5] Ludwig A, Tewes M, Glasmachers S, Löhndorf M and Quandt E 2002 High-frequency magnetoelastic materials for remote-interrogated stress sensors *J. Magn. Magn. Mater.* **242** 1126–31
[6] Shen W, Mathison L C, Petrenko V A and Chin B A 2009 Design and characterization of a magnetoelastic sensor for the detection of biological agents *J. Phys. D: Appl. Phys.* **43** 015004
[7] Xie F, Yang H, Li S, Shen W, Wan J, Johnson M L, Wikle H C, Kim D-J and Chin B A 2009 Amorphous magnetoelastic sensors for the detection of biological agents *Intermetallics* **17** 270–3
[8] Bravo IArnaiz Aand García-Arribas A 2018 Damping of magnetoelastic resonance for oil viscosity sensing *IEEE Trans. Magn.* **55** 1–5
[9] Ren L, Yu K and Tan Y 2019 Applications and advances of magnetoelastic sensors in biomedical engineering: a review *Materials* **12** 1135
[10] Sisniega B, Gutiérrez J and García-Arribas A 2021 Magnetoelastic resonance detection of calcium oxalate precipitation in low concentration solutions *IEEE Trans. Magn.* **58** 1–5
[11] Skinner W S, Zhang S, Guldberg R E and Ong K G 2022 Magnetoelastic sensor optimization for improving mass monitoring *Sensors* **22** 827
[12] Herzer G 2003 Magnetic materials for electronic article surveillance *J. Magn. Magn. Mater.* **254** 598–602
[13] Meyers K M and Ong K G 2021 Magnetoelastic materials for monitoring and controlling cells and tissues *Sustainability* **13** 13655
[14] Shekhar S, Karipott S S, Guldberg R E and Ong K G 2021 Magnetoelastic sensors for real-time tracking of cell growth *Biotechnol. Bioeng.* **118** 2380–5
[15] Le Bras Y and Greneche J M 2017 Magneto-elastic resonance: principles, modeling and applications *Resonance* vol 2 (London: IntechOpen) pp 13–34
[16] Peña A, Aguilera J D, Matatagui D, de la Presa P, Horrillo C, Hernando A and Marín P 2022 Real-time monitoring of breath biomarkers with a magnetoelastic contactless gas sensor: a proof of concept *Biosensors* **12** 871
[17] Saiz P G, Fernández de Luis R, Bartolome L, Gutiérrez J, Arriortua M I and Lopes A C 2020 Rhombic-magnetoelastic/metal–organic framework functionalized resonators for highly sensitive toluene detection *J. Mater. Chem.* C **8** 13743–53
[18] Cobeño A F, Zhukov A P, Pina E, Blanco J M, Gonzalez J and Barandiaran J M 2000 Sensitive magnetoelastic properties of amorphous ribbon for magnetoelastic sensors *J. Magn. Magn. Mater.* **215** 743–5
[19] Hernando A, Vázquez M and Barandiaran J M 1988 Metallic glasses and sensing applications *J. Phys. E: Sci. Instrum.* **21** 1129
[20] Sisniega B, Sagasti-Sedano A, Gutiérrez J and García-Arribas A 2020 Real time monitoring of calcium oxalate precipitation reaction by using corrosion resistant magnetoelastic resonance sensors *Sensors* **20** 2802
[21] Néel L 1950 Théorie du traînage magnétique des substances massives dans le domaine de Rayleigh *J. Phys. Radium* **11** 49–61
[22] Enz U 1958 Relation between disaccomodation and magnetic properties of manganese-ferrous ferrite *Physica* **24** 609–62
[23] Rivas J, López-Quintela M A, Martínez D, Walz F and Kronmüller H 1991 Magnetic relaxation in amorphous metals *J. Non-Cryst. Solids* **131** 1235–9
[24] Kwapuliński P and Haneczok G 2019 Magnetic relaxation in iron based melt spun ribbons *Acta Phys. Pol.* A **136** 701–4
[25] Kwapuliński P and Haneczok G 2020 Formation of the relaxed amorphous phase in iron-based amorphous alloys monitored by magnetic relaxation techniques *IEEE Trans. Magn.* **58** 1–7
[26] Kronmüller H 1983 Theory of magnetic after-effects in ferromagnetic amorphous alloys *Phil. Mag.* B **48** 127–50
[27] Allia P, Beatrice C and Vinai F 1990 A study of the dynamics of magnetic disaccommodation in amorphous ferromagnets. II. Theoretical considerations *J. Appl. Phys.* **68** 4724–7
[28] Knobel M, Sartorelli M L and Sinnecker J P 1997 Magnetoimpedance aftereffect in a soft magnetic amorphous wire *Phys. Rev.* B **55** R3362
[29] Sartorelli M L, Knobel M, Schoenmaker J, Gutierrez J and Barandiarán J M 1997 Giant magneto-impedance and its relaxation in Co–Fe–Si–B amorphous ribbons *Appl. Phys. Lett.* **71** 2208–10
[30] Sagasti A, Palomares V, Porro J M, Orúe I, Sánchez-Ilárduya M B, Lopes A C and Gutiérrez J 2020 Magnetic, magnetoelastic and corrosion resistant properties of (Fe–Ni)-based metallic glasses for structural health monitoring applications *Materials* **13** 57
[31] Lasheras A, Gutiérrez J, Balza A, Barandiarán J M and Rodríguez Pierna A 2014 Radiofrequency magnetoelastic resonators for magnetoelectric applications *J. Phys. D: Appl. Phys.* **47** 315003
[32] Lasheras A, Gutiérrez J and Barandiaran J M 2016 Quantification of size effects in the magnetoelectric response of metallic glass/PVDF laminates *Appl. Phys. Lett.* **108** 222903
[33] Sagasti A, Gutiérrez J, Lasheras A and Barandiaran J M 2019 Size dependence of the magnetoelastic properties of metallic glasses for actuation applications *Sensors* **19** 4296
[34] Sisniega B, Gutiérrez J, Muto V and García-Arribas A 2020 Improved determination of Q quality factor and resonance frequency in sensors based on the magnetoelastic resonance through the fitting to analytical expressions *Materials* **13** 4708
[35] Wang Y *et al* 2021 Long-time magnetic relaxation in antiferromagnetic topological material EuCd2As2 *Chin. Phys. Lett.* **38** 077201
[36] Allia P, Beatrice C, Vinai F, Knobel M and Turtelli R S 1991 Suppression of the magnetic-permeability relaxation in nanocrystalline Fe73. 5Cu1Nb3Si13. 5B9 *Appl. Phys. Lett.* **59** 2454–6

[37] Williams G and Watts D C 1970 Non-symmetrical dielectric relaxation behaviour arising from a simple empirical decay function *Trans. Faraday Soc.* **66** 80–85
[38] Allia P, Beatrice C and Vinai F 1993 The role of magnetoelastic coupling on magnetic disaccomodation of amorphous and nanocrystalline alloys *First Int. Meeting on Magnetoelastic Effects and Applications* (Elsevier) pp 47–55
[39] Rezende A, Turtelli R S and Missell F 1987 Magnetic permeability after-effect and the transition from Co-rich to Fe-rich amorphous alloys *IEEE Trans. Magn.* **23** 2128–30
[40] García-Arribas A, Barandiaran J M, Gutiérrez J and Sagastabeitia I 1997 On the origin of the nonlinear and chaotic behavior of the magnetoelastic resonance *J. Appl. Phys.* **81** 5686–8
[41] Hubert A and Schäfer R 2008 *Magnetic Domains: The Analysis of Magnetic Microstructures* (Berlin: Springer) (https://doi.org/10.1007/978-3-540-85054-0)
[42] Tsukahara S, Satoh T and Tsushima T 1978 Magnetic anisotropy distribution near the surface of amorphous ribbons *IEEE Trans. Magn.* **14** 1022–4
[43] Kronmüller H 1979 Micromagnetism in amorphous alloys *IEEE Trans. Magn.* **15** 1218–25